CALCULATION OF THE PRIMARY CURRENT DISTRIBUTION IN CELLS WITH CURVED ELECTRODES USING THE FINITE DIFFERENCE, CONSERVATIVE SCHEME, AND FINITE ELEMENT METHODS

Josip ZORIC[1] and Ivo ROUSAR

Prague Institute of Chemical Technology, Department of Inorganic Technology, 166 28 Prague 6, Czech Republic; e-mail: [1] zoricj@vscht.cz

Received April 17, 1996
Accepted July 18, 1996

The primary current distribution was calculated in cells with a curvilinear shape of the electrodes by the finite difference (FDM), the conservative scheme (CS), and the finite element methods (FEM). These methods were used for the solutions of the Laplace equation (LE) for a 2D cross-section of a cell consisting of two concentric cylinders (tubes) as electrodes and the inter-electrode space filled with electrolyte. For this cell the analytical solution of LE is known. The local current density on the approximated shape of the electrodes was calculated. The error in the normalized local current density relative to the mean was 5.2%, 52% or 0.2% with FDM using a 64×64 mesh, CS using 64×64 mesh or FEM using 969 nodes, respectively. Also the boundary element method (BEM) has been used. With 199 elements at the electrode the error in the normalized current density was 0.2%. Taking into account the simplicity of programming and the possibility of using previously developed modules in other calculations, FEM and BEM showed the best performance.
Key words: Primary current distribution; Curved electrodes; Numerical methods.

One of the technically important problems in electrochemistry is to find the local current density (*cd*) on electrodes, which have curvilinear boundaries of irregular shape. The shape of the cell is usually so complicated that it is not possible to find a convenient mathematical transformation of coordinates, which will simplify the calculation of the Laplace equation (LE) in the inter-electrode space[1]. One example is the aluminium electrowinning cell, which has two curvilinear boundaries, one of which is the anode, the second one is the shape of the frozen cryolite ledge[1,2]. A similar case is met in lead acid batteries with tubular lead dioxide electrodes treated by Landfors and Simonsson[3], and the authors also mentioned problems with the approximation of the curved boundary.

The curvilinear boundaries are approximated in different ways for different methods, as recommended in the literature concerning FDM, CS, and FEM (refs[1,2,4–6]). These approximations may lead to a change in the length of the curvilinear boundary and thus the average *cd* may change considerably. Also the local values of *cd* depend on the approximation of the boundary. The problem of discontinuities of the local values of *cd* on rounded corner of electrodes using FDM was observed for the case of primary cur-

rent distribution by Prentice and Tobias[7]. To solve the problem, lest square smoothing was performed over the electrode surface, which was divided into several parts. They were smoothed separately and then joined by splicing functions. Because both questions are of technical importance and no comparative analysis has been found in the literature, this study is an attempt to fill the mentioned gap.

RESULTS AND DISCUSSION

The Solution of LE for the 2D Cross-Section of the Cylindrical Cell

To test the above-mentioned methods, a cell with two symmetrical cylindrical electrodes of radius r_0 and r_1 was used with the electrolyte occupying the space between the outer and inner cylinders. One quarter of the 2D cross-section of the cell is considered, see Fig. 1. For the inter-electrode space filled with an electrolyte of resistivity ρ (conductivity κ), the Laplace equation (*1*) is valid. (In this study $\rho = 1\ \Omega$ cm, $\kappa = 1\ \Omega^{-1}\ \mathrm{cm}^{-1}$)

$$\nabla^2\varphi = 0 \tag{1}$$

In a polar coordinate system, Eq. (*1*) takes the form:

$$\frac{\partial^2\varphi}{\partial r^2} + \frac{1}{r}\frac{\partial\varphi}{\partial r} = 0\ . \tag{2}$$

The analytical solution of Eq. (*2*) is given by

$$\varphi = A_c \ln r + B_c\ . \tag{3}$$

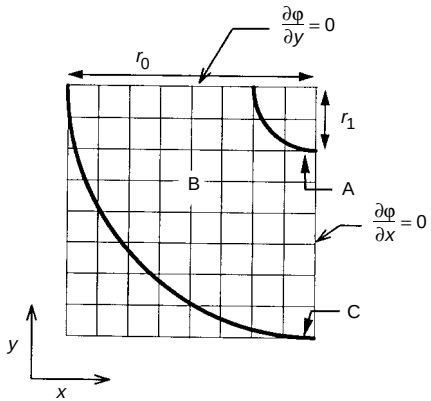

FIG. 1
The shape of the 2D cell with tubular anode and cathode. A anode with potential $\varphi(r_1) = 1.0$ V, C cathode with potential $\varphi(r_0) = 0.0$ V, B inter-electrode space in which LE was solved. For all cases $r_1 = 16$ cm, $r_0 = 64$ cm

The parameters A_c, and B_c can be determined from the boundary conditions valid for the case of unpolarized electrodes, i.e. primary current distribution:

$$\varphi(r_0) = 0.0 \text{ V} \ , \qquad \varphi(r_1) = 1.0 \text{ V} \ . \tag{4a,b}$$

From these boundary conditions the following coefficients are obtained:

$$A_c = \frac{1}{\ln \dfrac{r_1}{r_0}} \ , \tag{5}$$

$$B_c = -\frac{\ln r_0}{\ln \dfrac{r_1}{r_0}} \ . \tag{6}$$

For the potential φ in the inter-electrode space we have:

$$\varphi(r) = \frac{1}{\ln \dfrac{r_1}{r_0}} \ln \frac{r}{r_0} \ . \tag{7}$$

The local *cd* in the radial (normal) direction is defined as

$$j(r) = -\kappa \left(\frac{\partial \varphi}{\partial r} \right)_r \ . \tag{8}$$

The cathodic $j(r_0)$ and anodic *cd*s $j(r_1)$ are given

$$j(r_0) = \frac{-\kappa}{\ln \dfrac{r_1}{r_0}} \frac{1}{r_0} \ , \qquad j(r_1) = \frac{-\kappa}{\ln \dfrac{r_1}{r_0}} \frac{1}{r_1} \ . \tag{9a,b}$$

The theoretical value of the current I_{th} is then:

$$I_{th} = \frac{-2\pi\kappa}{\ln \dfrac{r_1}{r_0}} \ . \tag{10}$$

Definition of Quantities Used for the Description of the Results

By all methods, the values of the potentials were obtained in the inter-electrode space. From these values the *cd* at the electrode was calculated. With CS the current density normal to the boundary was evaluated as

$$j_i = I_i / l_i^* \ , \tag{11}$$

where l_i^* represents the length of the unit rectangle (h) or its diagonal ($h\sqrt{2}$) in the mesh, see Fig. 3.

With FEM and FDM normal *cd* to the boundary was evaluated in each node lying on the boundary by using a first-order approximation with error O(h). The normalized *cd* at the cathode is equal to

$$j_{\mathrm{n},i} = \frac{j_i}{j(r_0)} \ , \qquad i = 1, 2, \ldots, N \tag{12}$$

and at the anode

$$j_{\mathrm{n},i} = \frac{j_i}{j(r_1)} \ , \qquad i = 1, 2, \ldots, N \ , \tag{13}$$

where N represents the number of units on the boundary. The mean normalized value of *cd* was defined by

$$\bar{j}_{\mathrm{n}} = \frac{1}{N} \sum_{i=1}^{N} j_{\mathrm{n},i} \frac{l_i^*}{\bar{l}^*} \ , \tag{14}$$

where $\bar{l}^*$ represents the average length of one unit, given by

$$\bar{l}^* = \frac{1}{N} \sum_{i=1}^{N} l_i^* \ . \tag{15}$$

The length of the approximated electrode boundary is

$$L^* = \sum_{i=1}^{N} l_i^* \ . \tag{16}$$

The normalized current at the electrode was calculated as

$$I_n = \bar{j}_n L_n \ , \tag{17}$$

where L_n is the boundary length normalized by the theoretical boundary length L_{th}:

$$L_n = \frac{L^*}{L_{th}} \ . \tag{18}$$

The standard deviation (σ) of the normalized *cd* is given as

$$\sigma = \left(\frac{1}{N-1} \sum_{i=1}^{N} (j_{n,i} \frac{l_i^*}{\bar{l}_*} - \bar{j}_n)^2 \right)^{1/2} \ . \tag{19a}$$

The error (in %) of the normalized *cd* ($\bar{j}_n$) is for $N > 6$ equal to

$$\varepsilon = \pm 2\sigma \ 100 \ . \tag{19b}$$

The error (in %) of the normalized current (I_n) is defined by

$$\varepsilon = \pm \ |I_n - 1| \ 100 \ . \tag{19c}$$

Averaged *cd* over *p* units is given by

$$\bar{j}_{n,p,k} = \frac{1}{p} \sum_{i=i_1}^{i=i_2} j_{n,i} \ , \qquad i_1 = k - (p-1)/2 \ , \quad i_2 = k + (p-1)/2 \ . \tag{20}$$

Finite Difference Method

With the FDM the shape of the boundary was not changed, i.e. all the potentials of the anode were located at $r = r_1$ and all the potentials of the cathode were located at $r = r_0$ (Fig. 1). For a central point (i,j) the LE was approximated by

$$\left(\frac{\partial^2 \varphi}{\partial x^2} + \frac{\partial^2 \varphi}{\partial y^2} \right)_{i,j} = \frac{1}{h^2} (\varphi(i+1,j) + \varphi(i-1,j) + \varphi(i,j+1) + \varphi(i,j-1) - 4\varphi(i,j)) + O(h^2) \ . \tag{21}$$

If the surface of the electrode is represented by a smooth curve for a 2D cross-section, the approximation of the LE by Eq. (*21*) has an accuracy $O(h^2)$ (ref.[5]). For points (i,j) located near the boundary the following equation was used, valid for point A in Fig. 2.

$$\left(\frac{\partial^2\varphi}{\partial x^2}+\frac{\partial^2\varphi}{\partial y^2}\right)_A=\frac{1}{h^2}\left(\frac{\varphi_C}{a(1+a)}+\frac{\varphi_B}{1+a}+\frac{\varphi_E}{b(1+b)}+\right.$$

$$\left.+\frac{\varphi_D}{1+b}-\frac{(a+b)\varphi_A}{ab}\right)+O(h^2)\ . \qquad (22)$$

Depending on the shape of the boundary, different modes of Eq. (*22*) were developed, see Table I and refs[5,6]. The resulting matrix of coefficients is usually asymmetric, but

TABLE I
Values of the coefficients *a* and *b* used in Eq. (*22*) for different point types. See also Figs 2 and 3

Point type	φ_A	φ_B	*a*	*b*	Comment
1	0.0	0.0	*a*	*b*	
2	0.0	$\varphi(i+1,j)$	*a*	1	
3	$\varphi(i,j+1)$	0.0	1	*b*	
4	–	–	–	–	$\varphi(i,j)=0.0$
5	–	–	–	–	$\varphi(i,j)=1.0$
6	1.0	$\varphi(i-1,j)$	*a*	1	
7	$\varphi(i,j-1)$	1.0	1	*b*	

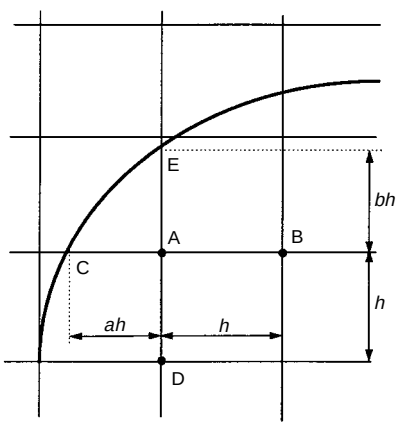

FIG. 2
The scheme of the curvilinear boundary and the points necessary for approximation by interpolation for FDM. See also Eq. (*22*)

there exist methods for obtaining a symmetric matrix[5,6]. The values of the coefficients *a* and *b* in Eq. (*22*) are given for different point types in Table I, as indicated in Figs 2 and 3.

Table II shows maximum and minimum values of the normalized *cd* obtained by the FDM, mean normalized value of *cd*, standard deviation of the normalized *cd* and the normalized current. From this table we can conclude that:

1. FDM is not a conservative method. FDM leads to different anode and cathode currents. By increasing the number of calculation points in the mesh the error in the normalized current decreases from 8.5% ($|0.9151 - 1| \cdot 100$) for an 8×8 mesh to 1.2% ($|0.9878 - 1| \cdot 100$) for a 64×64 mesh.

TABLE II
Normalized values of *cd*, $\bar{j}_n$, σ, and I_n, obtained by FDM. A anode; C cathode

Mesh dimensions	Electrode	j_{max}	j_{min}	$\bar{j}_n$	σ	I_n
8×8	C	1.0494	0.9876	1.0264	0.0507	1.0265
	A	0.9819	0.8482	0.9151	0.1336	0.9151
16×16	C	1.0309	1.0018	1.0166	0.0321	1.0166
	A	0.9975	0.9018	0.9547	0.0647	0.9547
32×32	C	1.0159	1.0005	1.0082	0.0215	1.0083
	A	1.0001	0.9437	0.9758	0.0441	0.9762
64×64	C	1.0079	1.0000	1.0039	0.0137	1.0039
	A	1.0000	0.9700	0.9878	0.0261	0.9878

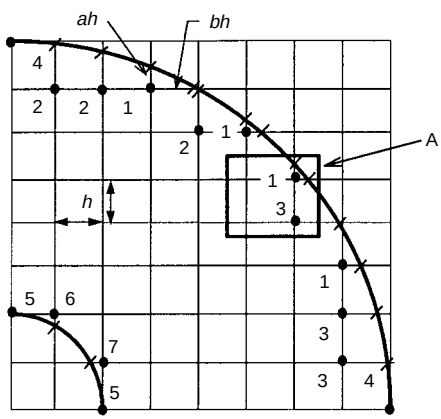

FIG. 3
Finite difference mesh 8×8 with the boundary point types 1 to 7. A rectangle covering points for the calculation of *cd* with $O(h^2)$ error at point 1, *h* nodes distance

2. The local values of normalized *cd* oscillate around the mean normalized *cd*, but the oscillations decrease considerably with increasing number of mesh points. For the 8 × 8 mesh the error in the local normalized *cd* was 26.6% (2 . 0.1336 . 100) and for the mesh of 64 × 64 points the error was only 5.2% (2 . 0.0261 . 100).

Local normalized current densities along the cathode obtained by FDM for the mesh with 64 × 64 calculation units are given in Fig. 4.

Conservative Scheme Method

The electrolytic cell shown in Fig. 1 was considered. The inter-electrode space was divided into rectangles and the electrodes were approximated by boundaries of rectangles. In the other case some parts of the electrodes were approximated by diagonals (Fig. 5). The boundaries for the 16 × 16 units are shown, but the calculation has also been carried out for 8 × 8 units, 32 × 32 units and 64 × 64 units. For more details about the method see refs[1,2]. The currents flowing in and out of the unit rectangle (*i*,*j*) are denoted according to Fig. 6 as $I_{k,l}$. The first subscript refers to the unit boundary line at which the current leaves the cell, and the second to the boundary line at which the current enters. For example, a current going from the boundary line $m = 1$ to the line $m = 2$ of the neighbouring unit is written as:

$$I_{1,2} = -\frac{\varphi(i-1,j) - \varphi(i,j) - A(i,j,1,2)}{\rho(i-1,j)\,\frac{d}{2d} + \rho(i,j)\,\frac{d}{2d}} \quad . \tag{23}$$

Equation (*23*) can be rewritten as:

$$I_{1,2} = -2\,\frac{\varphi(i-1,j) - \varphi(i,j) - A(i,j,1,2)}{\rho(i-1,j) + \rho(i,j)} \quad . \tag{24}$$

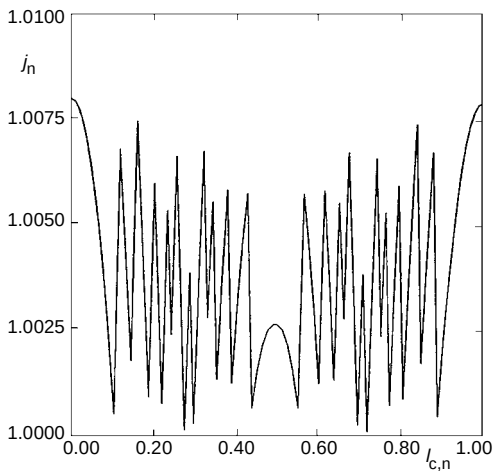

FIG. 4
Local normalized current densities along the cathode obtained by FDM. Mesh of 64 × 64 calculation units. j_n – Normalized local *cd* at the cathode, see also Eq. (*12*); $l_{c,n}$ – normalized cathode boundary length ($l_{c,n=0}$ at the beginning and $l_{c,n=1}$ at the end of the cathode)

Similar equations are valid for $I_{2,1}$, $I_{3,4}$ and $I_{4,3}$:

$$I_{2,1} = -2\,\frac{\varphi(i+1,j) - \varphi(i,j) - A(i,j,2,1)}{\rho(i+1,j) + \rho(i,j)}\ , \tag{25}$$

$$I_{3,4} = -2\,\frac{\varphi(i,j-1) - \varphi(i,j) - A(i,j,3,4)}{\rho(i,j-1) + \rho(i,j)}\ , \tag{26}$$

$$I_{4,3} = -2\,\frac{\varphi(i,j+1) - \varphi(i,j) - A(i,j,4,3)}{\rho(i,j+1) + \rho(i,j)}\ . \tag{27}$$

In Eqs (*23*) to (*27*), the terms $A(i,j,k,l)$ represent the voltage drop at the boundary between the sides k and l of the unit. This voltage drop is equal to the electrode potential at the electrode–electrolyte boundary. In the electrolyte, or in the electrode material, $A(i,j,k,l)$ is equal to zero. For the stationary state, the integral of the cd (j_n) normal to the surface (dS) along the boundary of the unit rectangle, must be equal to zero. This applies also for any closed surface or volume in the cell:

$$\oint j_n \, \mathrm{d}S = 0\ . \tag{28}$$

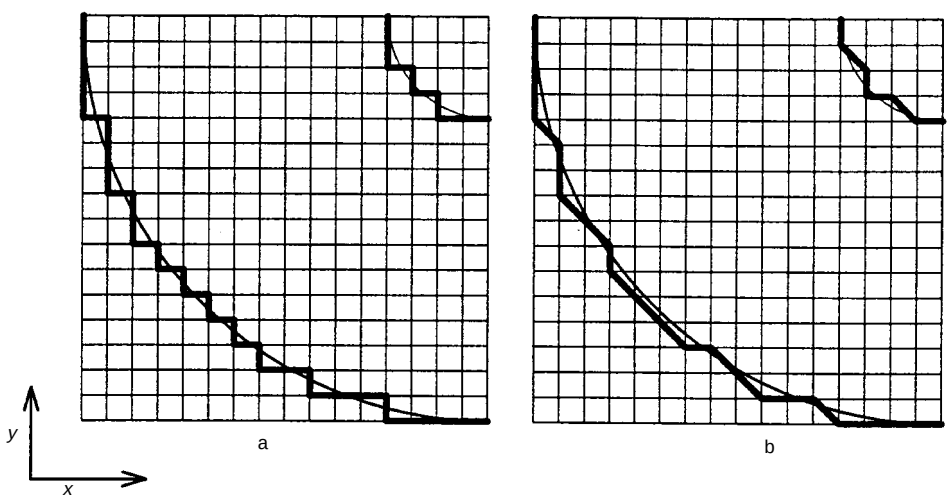

FIG. 5

CS method. Curved anode boundary approximation using two methods: a boundaries formed by rectangles, b boundaries formed by the combination of rectangles and diagonals. Mesh of 16 × 16 units

Equations (*24*) to (*27*) are used for the evaluation of Eq. (*28*). Alternatively, Eq. (*29*) can also be used,

$$I_{1,2} + I_{2,1} + I_{3,4} + I_{4,3} = 0 \quad . \tag{29}$$

On the basis of Eqs (*28*) and (*29*) the residuum $R(i,j)$ can be introduced:

$$R(i,j) = 2\left[\frac{\varphi(i-1,j) - \varphi(i,j)}{\rho(i-1,j) + \rho(i,j)} + \frac{\varphi(i+1,j) - \varphi(i,j)}{\rho(i+1,j) + \rho(i,j)} + \right.$$

$$\left. + \frac{\varphi(i,j-1,) - \varphi(i,j)}{\rho(i,j-1) + \rho(i,j)} + \frac{\varphi(i,j+1) - \varphi(i,j)}{\rho(i,j+1) + \rho(i,j)}\right] . \tag{30}$$

Equation (*30*) is valid for the electrolyte or electrode material, where the terms $A(i,j,k,l)$ are set equal to zero; it is satisfied if for all the points (i,j) in the 2D space

$$R(i,j) = 0 \quad , \qquad i, j \in \Omega \quad . \tag{31}$$

Equation (*29*) represents the so-called conservative scheme for the calculation of Galvani potentials in the considered space. ("Conservative" means that all the current flowing into the cell also flows out.) The conservative scheme with residuum $R(i,j)$ given by Eq. (*30*) also fulfills the LE for a space with changing resistivity.

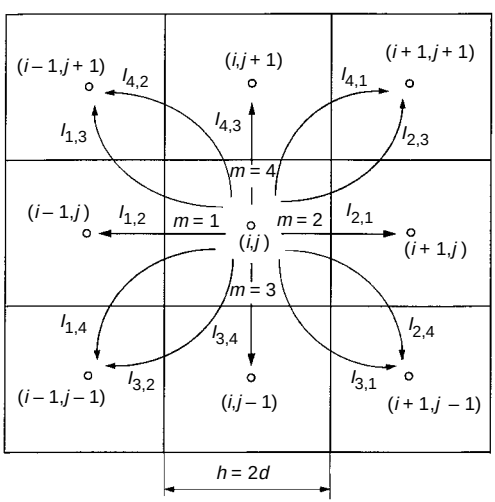

FIG. 6
CS method. Notation of currents for a rectangular grid in 2D space. The fluxes are denoted as I and the indices follow the notation of boundaries. Boundary indices of the calculation unit are denoted as m

$$\nabla\left(\frac{1}{\rho}\nabla\varphi\right) = 0 \qquad (32)$$

Equation (*32*) can generally be approximated in such a way that the conservation of current is not preserved. The most often used approach which is not conservative is FDM.

The curved boundaries were approximated by using: (i) a boundary of rectangular elements, (ii) boundaries formed by a combination of rectangular and diagonal elements (diagonal approximation of the boundary)[8]. In Fig. 6, all the possible fluxes are denoted, which may be used if rectangular or diagonal boundaries exist outside the (*i*,*j*) unit. For the case of rectangular boundaries Eq. (*29*) is valid. For the case of a unit cell with diagonal boundaries in Fig. 7, the analogy of Eq. (*29*) should be written as:

$$I_{1,2} + I_{3,4} + I_{2,3} + I_{4,1} + I_{2,4} + I_{4,2} = 0 \ . \qquad (33a)$$

For the fluxes $I_{4,2}$ and $I_{2,4}$, denoted by the dotted arrows in Fig. 7, the following formulae are valid:

$$I_{4,2} = \frac{\varphi(i-1,j+1) - \varphi(i,j)}{\rho(i-1,j+1) + \rho(i,j)} \ , \qquad (33b)$$

$$I_{2,4} = \frac{\varphi(i+1,j-1) - \varphi(i,j)}{\rho(i+1,j-1) + \rho(i,j)} \ . \qquad (33c)$$

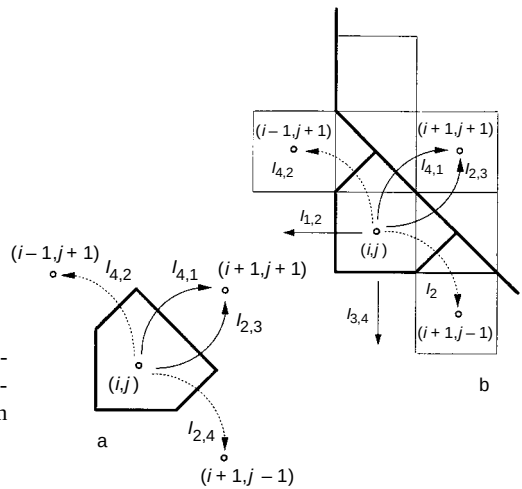

FIG. 7
Curved boundary approximation using diagonal boundary: a the shape of the diagonal element, b position of the diagonal element in the mesh and its fluxes

In Table III the results of the calculation of the normalized local *cd* at the boundaries of the electrodes by CS are shown. The calculations were carried out by using four meshes with 8 × 8, 16 × 16, 32 × 32, and 64 × 64 units, and rectangular and diagonal approximations of the curvilinear boundary. The results for both electrodes are given. For the mesh of 64 × 64 units, the normalized local *cd* along the cathode for both approximations are given in Figs 8 and 9. Averaging of the normalized *cd* was also carried out, and the obtained results for $p = 5$ units (window widths) are given in Figs 10 and 11. The averaging improved the local normalized *cd* values to a small extent. However, the length of the averaging interval (or the *p* number), for which the errors are restricted to 2%, represents the whole length of the cathode. Large *p* numbers are not suitable for an irregularly shaped curvilinear boundary, because usually the geometry will not be uniform and continuous as in the studied case. This means that large errors

TABLE III
Normalized values of *cd*, $\bar{j}_n$, σ, and I_n, obtained by CS. A anode; C cathode

Mesh dimensions and boundary aprox. type	Electrode	j_{max}	j_{min}	$\bar{j}_n$	σ	I_n	L_n
8 × 8	A	1.2358	0.5414	0.7625	0.2672	0.9709	1.2732
Rectangular	C	0.9813	0.5437	0.7625	0.2562	0.9709	1.2732
16 × 16	A	1.4084	0.5310	0.7950	0.2674	1.0123	1.2732
Rectangular	C	1.0951	0.5993	0.7950	0.2236	1.0123	1.2732
32 × 32	A	1.3812	0.4916	0.7980	0.2798	1.0161	1.2732
Rectangular	C	1.1752	0.4997	0.7980	0.2440	1.0161	1.2732
64 × 64	A	1.3432	0.4893	0.7895	0.2697	1.0053	1.2732
Rectangular	C	1.2385	0.4666	0.7895	0.2533	1.0053	1.2732
8 × 8	A	1.1974	0.5436	0.9791	0.2637	1.0183	1.0401
Diagonal	C	0.9902	0.8995	0.9371	0.1348	1.0183	1.0867
16 × 16	A	1.3292	0.5391	0.9209	0.2765	0.9793	1.0634
Diagonal	C	1.0314	0.6247	0.9012	0.2700	0.9793	1.0867
32 × 32	A	1.3259	0.5428	0.9477	0.2636	0.9967	1.0518
Diagonal	C	1.1380	0.6110	0.9583	0.2400	0.9967	1.0401
64 × 64	A	1.2889	0.5348	0.9528	0.2591	1.0221	1.0518
Diagonal	C	1.1334	0.5539	0.9635	0.2512	1.0221	1.0401

(20%) in local normalized *cd* can be expected, even when some reasonable averaging of the *cd* is employed.

The following conclusions about CS are worth mentioning:

1. When the electrode boundaries are approximated by a boundary of rectangles, the ratios of the maximum and minimum values of the local normalized *cd* to the theoretical one reached 1.41 and 0.466. The *cd* values did not tend to become more uniform with increasing number of units in the mesh. The mean normalized current density is approximately 76–80% of the theoretical value, due to the increase of the length of the boundary used in comparison with the theoretical; L_n is 1.27.

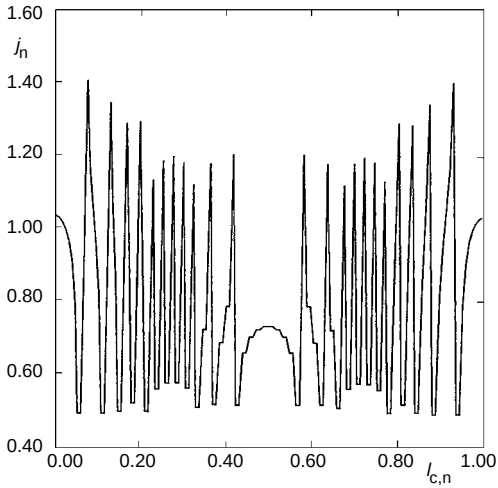

FIG. 8
Normalized local values of *cd* (j_n) along the normalized cathode boundary ($l_{c,n}$). CS rectangular boundary approximation; mesh 64 × 64

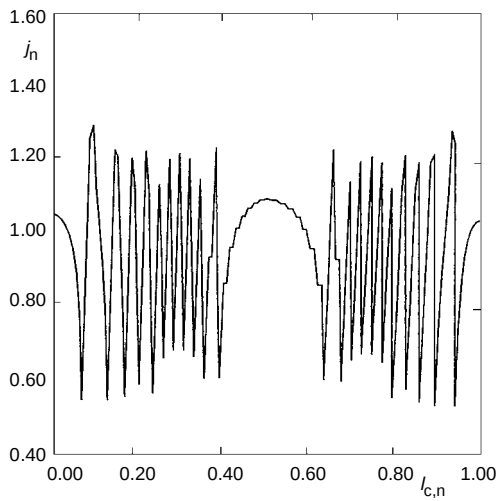

FIG. 9
Normalized local values of *cd* (j_n) along the normalized cathode boundary ($l_{c,n}$). CS diagonal boundary approximation; mesh 64 × 64

2. When the electrode boundaries are approximated by a boundary of rectangles and diagonals, the ratios of the maximum and minimum values of the normalized local *cd* to the theoretical reached 1.33 and 0.53. These values did not tend to become more uniform with an increasing number of units in the mesh. The mean normalized current density is close to the theoretical value, i.e. 0.90 up to 0.98. This is due to a good approximation of the boundary; L_n changes between 1.04 and 1.08. The error of the calculated potentials $\varphi(r)$ is about 50% of the theoretical value near the boundaries, but at a distance of 3 units from the boundaries the error in $\varphi(r)$ falls down to about 1%, and in the middle of the cell it is below 0.2% for the 64 × 64 mesh. The different approximations of the curvilinear boundary create different cell geometries, which re-

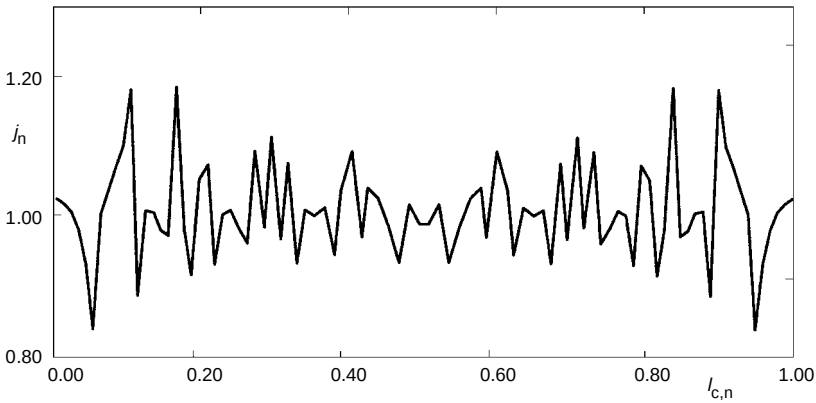

FIG. 10
Normalized local *cd* (j_n) at the normalized cathode boundary ($l_{c,n}$) after averaging with p = 5. CS rectangular boundary approximation; mesh 64 × 64

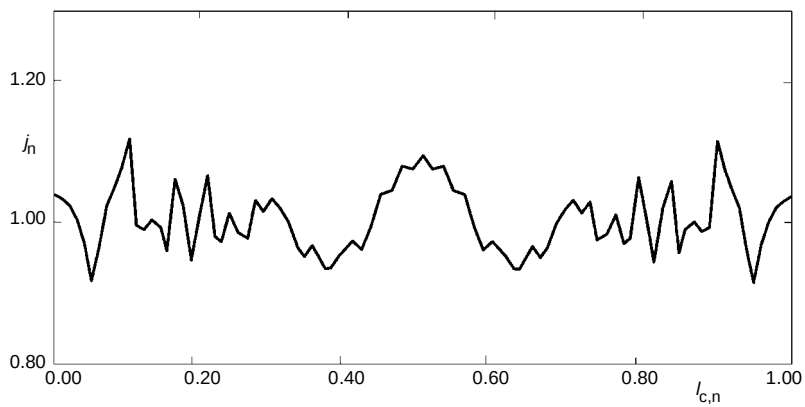

FIG. 11
Normalized local *cd* (j_n) at the normalized cathode boundary ($l_{c,n}$) after averaging with p = 5. CS diagonal boundary approximation; mesh 64 × 64

sult in different error distributions, see Figs 8 and 9. The cathode length used in Figs 8 and 9 is referred to the theoretical length of the whole cathode.

Finite Element Method

The interelectrode space (Fig. 1) was divided into triangular elements by selecting points on the boundaries (electrodes) as shown in Fig. 12. The transformation of the boundary problem to a variational formulation in Galerkin's form[1,4] was done for the Laplace equation written in x, y coordinates:

$$\frac{\partial^2\varphi}{\partial x^2} + \frac{\partial^2\varphi}{\partial y^2} = 0 \ , \qquad x, y \in \Omega \ , \tag{34}$$

valid for constant ρ. The essential boundary condition was applied to the anode and cathode boundary, denoted as Γ_1.

$$\varphi = \overline{\varphi}(x,y) \ , \qquad \text{on } \Gamma_1 \ . \tag{35}$$

On insulated surfaces Γ_2, the normal component of the current is prescribed

$$j_n = -\kappa \frac{\partial\varphi}{\partial x} = 0 \ \text{ or } \ j_n = -\kappa \frac{\partial\varphi}{\partial y} = 0 \ \text{ on } \ \Gamma_2 \ , \tag{36}$$

corresponding to the nonessential boundary condition. Consequently:

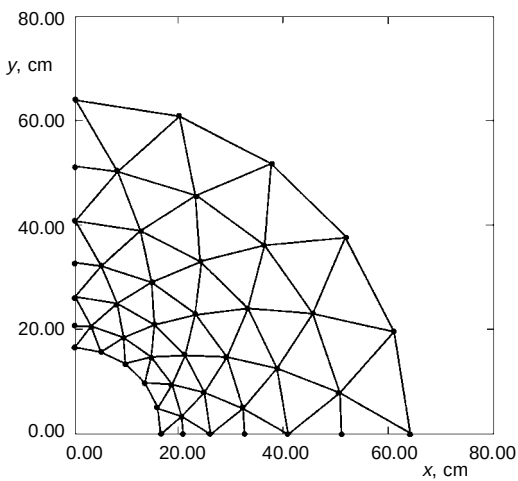

FIG. 12
The finite element calculation mesh. 45 nodes and 66 triangles

$$\Gamma = \Gamma_1 + \Gamma_2 \ . \tag{37}$$

By using the Galerkin's variational statement and rearranging the weighted integral of the residual using Green's theorem, the variational formulation of Eq. (*34*) was obtained in the form:

$$\iint \left(\frac{\partial \varphi^{(n)}}{\partial x} \frac{\partial \delta\varphi^{(n)}}{\partial x} + \frac{\partial \varphi^{(n)}}{\partial y} \frac{\partial \delta\varphi^{(n)}}{\partial y} \right) \mathrm{d}x\, \mathrm{d}y = -\int \frac{j_n}{\kappa} \delta\varphi^{(n)}\, \mathrm{d}\Gamma \ . \tag{38}$$

This formulation is suitable for the application of FEM. The elements and nodes were numbered to specify the element-node correspondence. Thus we obtain a system of equations which can be written in the following form:

$$\boldsymbol{M}^{(e)} \hat{\varphi}^{(e)} = \boldsymbol{F}^{(e)} \ , \qquad e \in \Omega \ , \tag{39}$$

where $\boldsymbol{M}^{(e)}$ is the characteristic matrix of the element and $\boldsymbol{F}^{(e)}$ is the vector of the right-hand sides. As a further step, Eqs (*39*) for all the elements were summed up giving the resulting matrix equation

$$\boldsymbol{M}\, \hat{\varphi} = \boldsymbol{F} \ . \tag{40}$$

The matrix of the system is denoted as $\boldsymbol{M}$ and the unknown system nodal vector as $\hat{\varphi}$. All the nodes in the given domain Ω are now referred to by the global numbering system from *l* to *m*, where *m* is the total number of nodes in Ω. Firstly the essential boundary conditions are introduced, then the system of linear equations has to be solved to obtain the vector $\hat{\varphi}$ for all nodal points. For more details, see refs[1,4].

In Table IV, the maximum and minimum values of the normalized *cd* obtained with the FEM are given. The following conclusions follow from Table IV and Fig. 13:

1. The FEM is not conservative, which means that the total current on the anode is not the same as the total current on the cathode. The deviations of the calculated normalized current from the theoretical were ±15%, at a low number of nodes equal to 27. They tend to zero, when the number of nodes increases. For 969 nodes the error in the total normalized current was only ±2.1%.

2. The error in the local normalized *cd* was ±1.2% for 27 nodes, and it decreased with an increasing number of nodes. For 969 nodes, the error in the local normalized *cd* was only 0.24%. As shown in Fig. 13, only small changes in the local *cd* appear at the

ends of the cell space, where nonequilateral triangles were used. By avoiding the use of nonequilateral triangles a very high accuracy can be achieved.

3. The approximation of the shape of the boundary by triangles can be very close to the theoretical boundary. For 27 nodes, L_n was 0.9935, and for 969 nodes it was 0.9998. For more information on the methods used in the present work see Appendix.

Boundary Element Method

Also the boundary element method[9] (BEM) with constant elements has been used for the solution of the Laplace equation in 2D. This numerical method calculates only the unknowns at the boundary of the domain, requesting additional calculations to get the values of the potential and *cd* in the domain[9]. It is possible to use advantages of the combination of the BEM and FEM (ref.[10]).

TABLE IV
Normalized values of *cd*, $\bar{j}_n$, σ, and I_n, obtained by FEM. A anode; C cathode

Number of nodes and triangles	Electrode	j_{max}	j_{min}	$\bar{j}_n$	σ	I_n
27 nodes	C	0.8613	0.8518	0.8572	0.0039	0.8572
36 triangles	A	1.1654	1.1531	1.1584	0.0056	1.1584
45 nodes	C	0.8897	0.8811	0.8861	0.0033	0.8861
66 triangles	A	1.1297	1.1191	1.1235	0.0044	1.1235
149 nodes	C	0.9448	0.9399	0.9435	0.0017	0.9435
252 triangles	A	1.0626	1.0572	1.0586	0.0020	1.0586
313 nodes	C	0.9632	0.9597	0.9625	0.0010	0.9625
558 triangles	A	1.0413	1.0377	1.0384	0.0012	1.0384
969 nodes	C	0.9795	0.9775	0.9792	0.0005	0.9792
1 815 triangles	A	1.0207	1.0164	1.0204	0.0012	1.0204

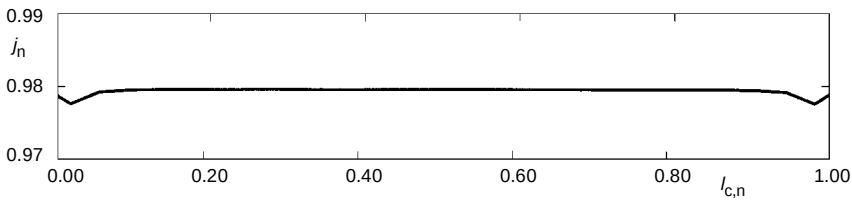

FIG. 13
Normalized local current densities (j_n) along the normalized cathode boundary ($l_{c,n}$) obtained by FEM Mesh with 969 nodes

The results obtained by the use of the BEM were very similar to those obtained with the FEM. With 199 boundary elements on the cathode, the error in the normalized *cd* was 0.2% (but the number of unknowns was only 4×199). In Fig. 14 the normalized current density along the cathode, calculated using the BEM, is shown.

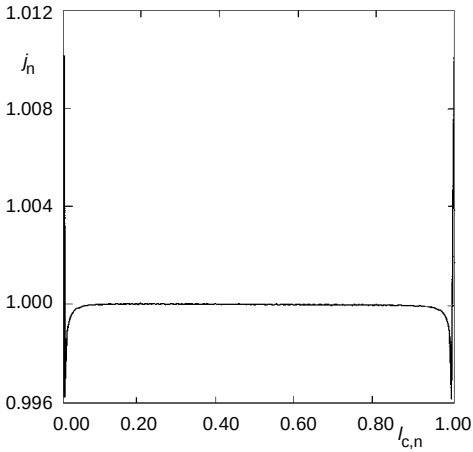

FIG. 14
Normalized local current densities (j_n) along the normalized cathode boundary ($l_{c,n}$) obtained by BEM. 199 constant elements at the cathode boundary (4×199 unknowns in the whole cell).

CONCLUSIONS

For the cells with primary current distribution and curved electrode boundaries studied in this paper, the following recommendations for the use of FDM, CS, and FEM can be made:

Firstly, FEM is recommended because of low errors, less than 0.2% in the normalized local *cd*, using approximately 1 000 nodes in the inter-electrode space. The method can be easily programmed. Mesh generators, which minimize the number of nonequilateral triangles at the electrode boundary, should be used. The nonequilateral triangles are sources of local errors. The error in the local *cd* decreases with increasing number of triangles and with the use of nearly equilateral triangles. Developed modules can be used in different calculations.

Secondly, FDM leads to small errors, less than 5.2%, in the normalized local *cd*, with a 64×64 mesh. The error decreases with increasing number of points in the mesh. Two neighbouring points may have errors of different signs in the local *cd*. The normalized local *cd* differs by one to two per cent from the mean normalized *cd*.

Thirdly, the CS methods lead to high errors in the local *cd* (approximately 50%), and these errors change sign for two neighbouring rectangles. When increasing the number of points in the mesh, the errors in the local *cd* are not damped appreciably. Hence, this method cannot be recommended for curved electrode boundaries.

APPENDIX

For a cell that has curvilinear electrode boundaries for which suitable mathematical transformation cannot be developed (see ref.[1]), approximations of the shape of these boundaries have to be used. Each of the above-mentioned methods has its own rules for the approximation of the curved boundary.

Finite Difference Method

The numerical approximations for the Laplace equation at calculation points along the boundary are significantly different from the formula valid for the bulk electrolyte (compare Eqs (*21*) and (*22*)). To take into account all possible cases, 7 point types have to be introduced, see Figs 2 and 3, and Table I.

The programming process should have the following steps:

1. Construction of the basic mesh system.

2. Determination of points close to the boundary and their types.

3. Determination of their distances from the boundary in both directions.

4. Definition of equation coefficients according to point types.

5. Solution of the resulting system of linear equations.

6. Calculating the current densities.

Two different methods can be used to calculate the current densities. The programming is easier when using a first-order approximation taking into account one mesh point and a value of the potential at the boundary. The second-order approximation uses nonequidistant local meshes for the calculation of *cd*. One of them is illustrated in Fig. 3. With a nonequidistant mesh, the method of undetermined coefficients can be used to develop the formulae in the *x* direction. The following formula is used for the local *cd*:

$$f^{(k)}(x) = \sum c_i f(x_i) + R(f) \quad . \tag{41}$$

The coefficients should be chosen in such a way as to obtain $R(f) = 0$. When $f = 1; x; x^2; x^3; \ldots; x^n$, a following system of linear algebraic equations is obtained.

$$c_0 + c_1 + c_n = 0$$

$$c_0 x_0 + c_1 x_1 + \ldots + c_n x_n = 0 \qquad \left(= \frac{\mathrm{d}^k}{\mathrm{d}x^k}(x) \,||_{x=\bar{x}}\right)$$

$$\ldots$$

$$c_0 x_0^{k-1} + c_1 x_1^{k-1} + \ldots + c_n x_n^{k-1} = 0$$

$$c_0 x_0^k + c_1 x_1^k + \ldots + c_n x_n^k = k! \qquad (= \frac{\mathrm{d}^k}{\mathrm{d}x^k}(x^k) \,||_{x=\bar{x}})$$

$$c_0 x_0^{k+1} + c_1 x_1^{k+1} + \ldots + c_n x_n^{k+1} = (k+1)\,!\,\bar{x}$$

$$\ldots$$

$$c_0 x_0^n + c_1 x_1^n + \ldots + c_n x_n^n = n(n-1)\ldots(n-k+1)\,!\,\bar{x}^{n-k} \qquad (42)$$

In the *y* direction the points for the calculation have to be obtained by interpolation using neighbouring points. The resulting *cd* is obtained as a vector summation of these two local current densities. This method is accurate but time consuming for programming. In Table II, the approximation of the first order, was used for the evaluation of the local *cd*.

Conservative Scheme

The numerical approximations for LE at calculation points along the boundary differ significantly from the formula valid for the bulk. The neighbouring four sides determine the flux (current density). To take into account all possible cases, 20 or more point types have to be introduced, depending on the shape of the boundary. The programming has the following steps:

1. Definition of the calculation mesh.

2. Discretization of the curvilinear boundaries.

3. Definition the point types in accordance with their position at the boundary.

4. Definition of the equation coefficients according to the point types and boundary/interface conditions.

5. The solution of the system of resulting linear equations, (Eq. (*30*) or similar).

6. Calculation of the current densities using special formulae different for each point type.

7. Calculation of the current integral for each unit along the surface (Eq. (*28*)) to check the preceding calculation.

A graphical interface for checking the boundary discretization is desirable, and this problem can be solved using existing graphic libraries provided with every modern FORTRAN, Pascal, and C compiler. The programming is time-consuming, though the computer requirements are not particularly high. All programs were written in MS FORTRAN 5.1, and a DX2 66 MHz computer with 12 MB RAM was used. For problems with larger meshes, UNIX network servers were employed. Successive relaxation method with memory pointers and compressed memory blocks were used, allowing large fields to be handled.

Finite Element Method

The FEM for a cell with a curvilinear boundary requires the development of several software modules. A mesh generator of triangles can easily be constructed in the case of geometrically defined shapes. Generating the mesh for complex cell shapes, however, becomes complex. To obtain a uniform and low error distribution in the whole cell or in the region of interest, it is necessary to use equilateral triangles, hence a special programming strategy. References about that can be found in the *Journal of Numerical Methods in Engineering*. For the calculation of the example treated in this paper we developed a special mesh generator. The mesh generators can be found on the market as part of the standard FEM software. Output of any commercial software can be taken if it has the following form: nodes with their indices and coordinates, and triangles with their nodes. Also, it is necessary to have the numbers of the triangles adjacent to the electrodes, and the electrode node numbers, necessary for the subroutines in which the calculation of the local *cd* is done. The other modules deal with the definition of the equation coefficients (Eqs (*39*) and (*40*)), the boundary conditions, the solution of the system of linear equations (Eq. (*40*)), the calculation of the local *cd* along the electrode boundaries, and the current flowing through the electrodes.

SYMBOLS

A_c, B_c	coefficients in theoretical solution, Eq. (*3*)
a, *b*	coefficients for LE approximation by FDM, Figs 2, 3, and Eq. (*22*)
d	dimension of rectangular CS calculation unit, Fig. 6
$\boldsymbol{F}$	vector of right-hand sides, Eqs (*39*) and (*40*)
h	dimension of the FDM and CS calculation units, Figs 2, 3, and 6
I	current
j	current density
l	length of electrode boundary unit, Eqs (*14*) and (*15*), and also length of the electrode boundary (depending on subscripts)
$\boldsymbol{M}$	matrix of coefficients, Eqs (*39*) and (*40*)
r, r_0, r_1	radii of cylinder, Fig. 1
R(i,j)	residuum, Eq. (*30*)
Γ, Γ_1, Γ_2	boundary curves for FEM, Eqs (*35*) and (*38*)
κ	conductivity
ρ	resistivity
σ	standard deviation, Eq. (*19*)
φ	potential
$\hat{\varphi}$	vector of potentials
Ω	integration domain, Eq. (*34*)
Subscripts	
A	anode
C	cathode
E	electrolyte
M	metal

n	normalized
th	theoretical value
Superscript	
e	triangular element, Eq. (*39*)

The authors thank to Prof. J. Thonstad (NTH, Trondheim, Norway) for his continuous interest and valuable discussions.

REFERENCES

1. Rousar I., Micka K., Kimla A.: *Electrochemical Engineering*, Vols 1 and 2. Elsevier, Amsterdam and Academia, Prague 1986.
2. Steffen B., Rousar I.: Electrochim. Acta *40*, 379 (1995).
3. Landfors J., Simonsson D.: J. Appl. Electrochem. *25*, 315 (1995).
4. Zienkiewicz O. C.: *The Finite Element Method in Engineering Science*. McGraw–Hill, London 1971.
5. Vitasek E.: *Numericke metody*. SNTL, Praha 1987.
6. Karnahan B., Luther H. A., Wilkes J. O.: *Applied Numerical Methods*. Wiley, New York 1969.
7. Prentice G. A., Tobias C. W.: J. Electrochem. Soc. *129*, 78 (1982).
8. Zoric J., Rousar I., Thonstad J., Kuang Z.: Unpublished results.
9. Brebbia C. A., Walker S.: *Boundary Element Techniques in Engineering*. Newnes–Butterworths, London 1980.
10. Walker S., Brebbia C. S. (Eds): *Proceedings of the 3rd International Seminar, Irvine, California 1981*. Springer, Berlin 1981.